Highly sensitive digital optical sensor with large measurement range based on the dual-microring resonator with waveguide-coupled feedback*

Xiang Xing-Ye(向星烨)†, Wang Kui-Ru(王葵如), Yuan Jin-Hui(苑金辉), Jin Bo-Yuan(晋博源), Sang Xin-Zhu(桑新柱), and Yu Chong-Xiu(余重秀)

State Key Laboratory of Information Photonics and Optical Communications, Beijing University of Posts and Telecommunications, Beijing 100876, *China*

(Received 14 June 2013; revised manuscript received 23 July 2013; published online 12 February 2014)

We propose a novel high-performance digital optical sensor based on the Mach–Zehnder interferential effect and the dual-microring resonators with the waveguide-coupled feedback. The simulation results show that the sensitivity of the sensor can be orders of magnitude higher than that of a conventional sensor, and high quality factor is not critical in it. Moreover, by optimizing the length of the feedback waveguide to be equal to the perimeter of the ring, the measurement range of the proposed sensor is twice as much as that of the conventional sensor in the weak coupling case.

Keywords: optical sensor, microring resonator, high sensitivity, large measurement range

PACS: 42.60.Da, 42.79.−e, 42.82.−m **DOI:** 10.1088/1674-1056/23/3/034206

1. Introduction

Sensors based on the microring resonators (MRRs) have extensive applications in the environmental and biological detections due to its high sensitivity and ultra-compact scale.[1–7] In an MRR sensor, the target analyte covering the surface makes a change in the refractive index of its cladding, which can be probed by the evanescent tail of the modal field, and thus the effective refractive index of the MRR changes. Consequently, the output spectral response will change. This change can be monitored by the intensity variation at the fixed wavelength or the resonance wavelength shift. Up to now, various methods have been developed to improve the two important figure of merit of MRR sensors: sensitivity and measurement range.

For the detection mechanism of intensity, the sensitivity is defined as the rate of change of a fixed wavelength's light intensity under a shift of the target analyte. Since quality factor Q can indicate the sharpness of the spectral resonance, the sensitivity depends heavily on Q.[8] To achieve a high sensitivity, the microring with a high Q can be obtained by choosing small coupling coefficient, minimizing the intrinsic loss,[9–11] and utilizing the special structures such as the concentric microring,[12] the dual microring,[4] and the Fano effect introduced constructions.[13,14] However, in these cases, high sensitivity is usually along with small measurement range, because with a sharp resonance peak, the response approaches zero very fast in a narrow bandwidth as the index changes. For the mechanism of spectrum, the higher sensitivity generally requires larger resonance shift. In this case, higher Q makes it easier to distinguish the resonances. Researchers have developed different methods to improve the sensitivity. Recently, a kind of highly sensitive sensor consisting of two cascaded MRRs has been proposed and then experimentally demonstrated,[15,16] where a high sensitivity can be obtained due to the Vernier effect. However, the measurement range is limited because of the dependence on the free spectrum range (FSR) of MRR. Even if a large FSR is achieved by reducing the radius, a smaller radius means higher radiation loss and thus a lower Q, which makes it difficult to detect the response. Though the MRR sensors with large measurement range have been realized via some special structures, such as the feedback-microring resonator (feedback-MRR) based structure,[17] the sensitivities in those cases are still as low as that of the conventional MRR sensors.

By means of the scheme of spectrum shift, a novel digital optical sensor with high sensitivity and large measurement range is studied in this paper. The structure is based on the Mach–Zehnder interferometer (MZI), where the two arms are replaced by the microrings with the feedback waveguide. The silicon-on-insulator (SOI) material is used to realize the device. Compared to the conventional MRR sensor, the proposed new sensor can be more sensitive. Since the resonance shift is usually on the nanometer scale, the detecting condition is not very rigorous. Moreover, the high Q factor is not critical in this sensor. By optimizing the length difference between the feedback waveguide and the ring in each part of MZI structure, a larger measurement range is obtained, which can be twice as much as that of the conventional sensor.

*Project supported by the National Basic Research Program of China (Grant No. 2010CB327601).

†Corresponding author. E-mail: xiangxingye0409@126.com

© 2014 Chinese Physical Society and IOP Publishing Ltd

2. Structure and theory

For an MRR sensor, when the refractive index of analyte changes, the spectral response will shift accordingly: $\Delta\lambda = \Delta n_{\rm eff}\lambda/n_{\rm eff}$, where $n_{\rm eff}$ is the effective index of the fundamental mode in the ring and $\Delta n_{\rm eff}$ is the change of $n_{\rm eff}$. The value of $\Delta n_{\rm eff}$ is almost proportional to the change $\Delta n_{\rm c}$ of the ambient refractive index:[4] $\Delta n_{\rm eff} = K\Delta n_{\rm c}$, where K is a constant depending on the material and waveguide cross section. Thus, the relationship between $\Delta\lambda$ and $\Delta n_{\rm c}$ is: $\Delta n_{\rm c} = \Delta\lambda n_{\rm eff}/K\lambda$. Since the resonance shift $\Delta\lambda$ should be smaller than its free spectral range FSR, the measurement range of the ambient refractive index can be obtained: $\Delta n_{\rm c} < {\rm FSR}n_{\rm eff}/K\lambda$, indicating the heavy dependence between measurement range and FSR. In addition to the measurement range, another important figure of merit of MRR sensor is sensitivity. It is always defined as:[8] $S_0 = \Delta\lambda/\Delta n_{\rm c} = (\Delta n_{\rm eff}/\Delta n_{\rm c})\Delta\lambda/\Delta n_{\rm eff} = KS$, where $S = \Delta\lambda/\Delta n_{\rm eff}$ is defined as the device sensitivity, and K is the waveguide sensitivity which is a constant in a certain waveguide structure. In the following, the device sensitivity and the measurement range are discussed in detail.

The sensing scheme based on the Mach–Zehnder (MZ) structure and dual MRs with a U-bend feedback waveguide is shown in Fig. 1(a), including the sensing ring (region i) and the reference ring (region ii). The region i senses the refractive index changes of analyte directly, while the region ii does not due to the up-cladding. At the input port, the light is launched into the sensing and reference rings through the 3-dB coupler, and the responses mutually interfere at the output port.

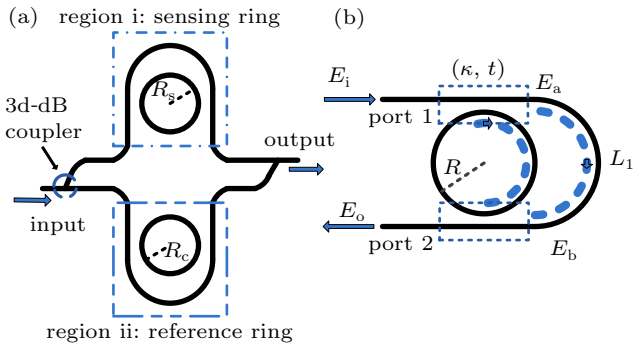


Fig. 1. (color online) Schematic of sensor based on MZI and dual MRs with the U-bend feedback waveguide. (a) The whole structure, and (b) the basic structure.

2.1. Transmission spectrum of basic structure

The transmission spectra of regions i and ii are used to analyze the response at the output port. Figure 1(b) shows the individual basic structure (feedback-MRR), which can describe the two regions (an MR with U-bend waveguide-coupled feedback). The transmission matrix method (TMM) is used to model this structure here.[18–20] The input and output coupling regions are shown in two dashed boxes, where κ and t (real numbers) are the coupling and self-coupling coefficients ($\kappa^2 + t^2 = 1$ for the lossless coupling). The $E_{\rm i}$ and $E_{\rm o}$ are the light fields of the port 1 and 2, and $E_{\rm a}$ and $E_{\rm b}$ are the light fields inside the U-bend waveguide after the input coupling region and before the output coupling region. The radius of MR is R, and the length of U-bend waveguide is L_1. The amplitude transmission factors for the ring and the feedback waveguide are $\tau = {\rm e}^{-2\pi R\alpha}$ and $\tau_1 = {\rm e}^{-L_1\alpha}$, where α is the loss coefficient. The phase changes for the half-circular ring and the feedback waveguide are $\theta = (2\pi^2/\lambda)n_{\rm eff}R$ and $\phi = (2\pi/\lambda)n_{\rm eff}L_1$, where $n_{\rm eff}$ is the effective refractive index of the waveguide and λ is the free space wavelength. The transmission matrix of the input and output coupling regions ($M_{\rm c}$) and the ring ($M_{\rm r}$) are given by

$$M_{\rm c} = (1/{\rm i}\kappa)\begin{bmatrix} -t & 1 \\ -1 & t \end{bmatrix}, \quad M_{\rm r} = \begin{bmatrix} {\rm e}^{-{\rm i}\theta/2}\tau^{-1/2} & 0 \\ 0 & {\rm e}^{{\rm i}\theta/2}\tau^{1/2} \end{bmatrix}, \tag{1}$$

the steady-state relationship between the field amplitude can be described as

$$\begin{bmatrix} E_{\rm o} \\ E_{\rm b} \end{bmatrix} = M_{\rm c}M_{\rm r}M_{\rm c}\begin{bmatrix} E_{\rm i} \\ E_{\rm a} \end{bmatrix}, \tag{2}$$

and the relationship between $E_{\rm a}$ and $E_{\rm b}$ is given by

$$E_{\rm b} = \tau_1 {\rm e}^{{\rm i}\varphi}E_{\rm a}. \tag{3}$$

Combining Eqs. (1)–(3), we can obtain the transmission spectrum at port 2 as

$$T = I_{\rm n} = \left|\frac{E_{\rm o}}{E_{\rm i}}\right|^2 = \left|\frac{{\rm e}^{{\rm i}\varphi}t^2\tau_1 - {\rm e}^{{\rm i}\theta}\tau^{1/2}\kappa^2 - {\rm e}^{2\theta{\rm i}}\,{\rm e}^{{\rm i}\varphi}\tau\tau_1}{1 - {\rm e}^{2\theta{\rm i}}t^2 + \kappa^2\tau_1\tau^{1/2}{\rm e}^{{\rm i}\theta}\,{\rm e}^{{\rm i}\varphi}}\right|^2. \tag{4}$$

In the weak coupling case ($t^2 \gg \kappa^2$), the spectrum of the feedback-MRR is like an inverted Lorentzian resonance line shape, which is similar to the spectrum of a single MR coupled with one straight waveguide. We make it possible to have only one resonance dip with a high extinction ratio (ER) within a larger wavelength span (quasi-FSR) by optimizing the length difference between the feedback waveguide and the ring and adjusting the coupling coefficient κ.[17,21] We find that the quasi-FSR of the spectrum will be twice the FSR of a typical single MRR when the length of the feedback waveguide is equal to the perimeter of the circle ring. The optimized spectra of the feedback MRR are shown in Figs. 2(a)–2(c) in the following part. Different radii of rings lead to different quasi-FSRs.

2.2. Spectral response at output port

The whole spectrum at the output port is based on the interference of two individual feedback MRRs' spectra. Figure 2 is used here to explain the sensing principle of the whole structure. We choose different radii: $R_{\rm s}$ for the sensing ring and $R_{\rm r}$ for the reference ring ($R_{\rm s} > R_{\rm r}$), so that they have different quasi-FSRs (quasi-FSR$_{\rm s}$ < quasi-FSR$_{\rm r}$). Their response spectra are shown in Figs. 2(a) and 2(c) when the sensing ring region does not have the analyte around. In this case, when one resonance wavelength of the sensing ring coincides with

one of the reference ring at λ_i (the overlap resonance wavelength), the phase difference between the light fields from two regions will be $2a\pi$ (a is an integer), thus the MZI structure will form a central resonance dip. When two non-overlapping resonances meet, symmetric transmission spectrum with the split dips around the central resonance will be generated.

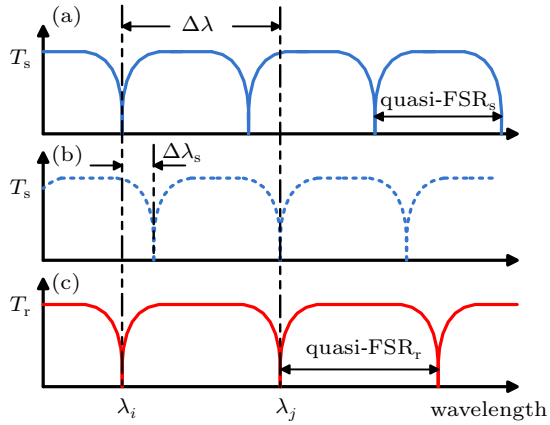


Fig. 2. (color online) Schematic diagram of the spectral response of (a) the sensing ring without analyte, (b) the sensing ring with analyte, and (c) the reference ring.

As shown in Fig. 2(b), the spectral response of the sensing ring will shift accordingly when the refractive index of analyte changes (in presence of analyte). At this time, two overlap resonance wavelengths will coincide at λ_j, which corresponds to the adjacent central resonance in the output spectrum. Thus, by detecting the shift of the central resonance dip (from λ_i to λ_j), we can obtain the index change of analyte. As seen from Fig. 2, the relationship between the shift of the output spectrum and that of the sensing ring's spectrum is defined as follows:

$$\Delta\lambda = \lambda_j - \lambda_i = \Delta\lambda_s + m\,\text{quasi-FSR}_s = n\,\text{quasi-FSR}_r, \quad (5)$$

where m and n are integers, $\Delta\lambda_s$ is the resonance shift of the sensing MRR, and $\Delta\lambda$ is the shift of the central resonance dip in the output spectrum. The spectral shift $\Delta\lambda$ is integral multiples of the reference feedback-MRR's quasi-FSR, which means that when the refractive index changes discretely, the central resonance dip will shift digitally. In such a digital way, when $\Delta\lambda_s$ satisfies the condition

$$\Delta\text{FSR}_Q < \Delta\lambda_s < \text{quasi-FSR}_r, \quad (6)$$

where $\Delta\text{FSR}_Q = \text{quasi-FSR}_r - \text{quasi-FSR}_s$, m and n will satisfy $m = n$. On the contrary, the relationship between m and n will be uncertain if $\Delta\lambda_s$ is too small or large. In order to gain the only refractive index of the analyte and to make correct interrogation, $\Delta\lambda_s$ should be in the range given by Eq. (6), corresponding to the measurement range. According to Eq. (5), the output spectrum shifts n quasi-FSR$_r$, so the minimum measurable index-change of analyte (Δn_{eff}) which corresponds to the minimum shift of the sensing ring's spectrum ($\Delta\lambda_s$) occurs for $n = 1$. From Eq. (6), it is found that the measurement range of the proposed sensor can be large since the quasi-FSR$_r$ of this sensor is larger than the FSR of conventional sensors. Thus, the sensitivity S can be obtained based on Eq. (5) as

$$S = \frac{\Delta\lambda}{\Delta n_{\text{eff}}} = \frac{\text{quasi-FSR}_r}{\Delta\text{FSR}_Q}\frac{\Delta\lambda_s}{\Delta n_{\text{eff}}} = F_a\frac{\Delta\lambda_s}{\Delta n_{\text{eff}}}, \quad (7)$$

where $\Delta\lambda_s/\Delta n_{\text{eff}}$ is the sensitivity of conventional sensors, and $F_a = \text{quasi-FSR}_r/\Delta\text{FSR}_Q$ is the improvement factor of the sensitivity. From Eq. (7), it is found that the sensitivity can be many times higher than that of a conventional sensor since the quasi-FSR$_r$ is much larger than ΔFSR_Q.

3. Simulation results and discussion

Firstly, we analyze the spectrum of the feedback MRR due to its strong effect on the output transmission spectrum. We choose the typical parameters of Si waveguides as 220 nm × 500 nm (height/width),[15] and the radius is defined as $r = 40.28$ μm (with a low bending loss). Assuming that the length of the feedback waveguide is equal to the perimeter of the ring, and the input light field is normalized ($|E_i|^2 = 1$). Figure 3(a) shows the spectral responses of feedback MRR and the comparable single MR coupled with straight waveguide, and we choose $\kappa = 0.15$ for the weak coupling.

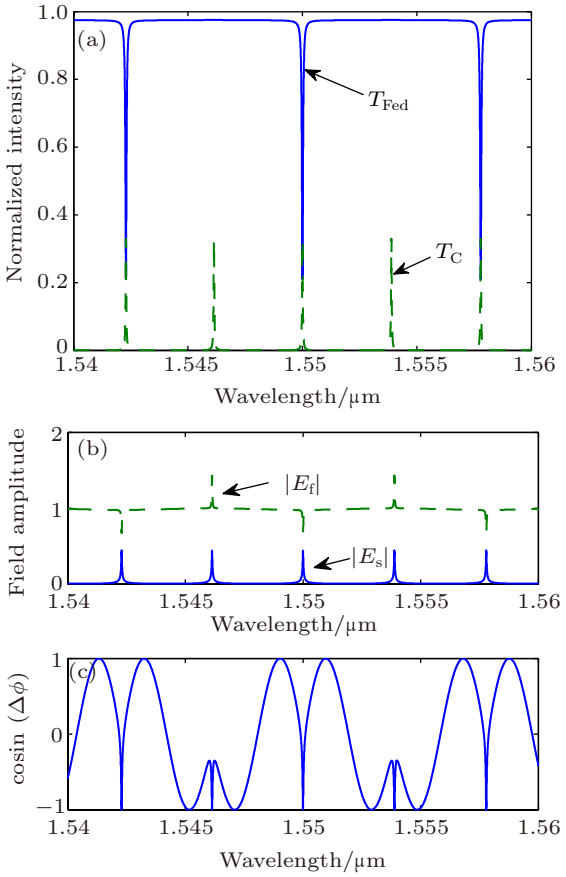


Fig. 3. (color online) (a) Spectral response of the feedback MRR (T_{Fed}) in comparison to a typical single-ring add-drop MRR (T_C); (b) amplitude of the feedback-interferential light field ($|E_f|$) and the single MR ($|E_s|$), and (c) the phase difference.

From Fig. 3(a), it can be seen that the quasi-FSR of feedback-MRR is twice as much as the FSR of a typical single-ring add-drop MRR. In order to analyze this phenomenon, we take the spectral output response of feedback-MRR as interference between two parts

$$|E_{\text{out}}|^2 = |E_{\text{s}}|^2 + |E_{\text{f}}|^2 + 2|E_{\text{s}}||E_{\text{f}}|\cos(\Delta\Phi).$$

The $|E_{\text{s}}|$ part is like the light field of a typical single-ring add-drop MR's drop port, and the $|E_{\text{f}}|$ part is like the feedback-interferential light field which pass through the U-bend feedback waveguide. Figures 2(b) and 2(c) show the amplitude of the two light fields and the phase difference. As seen from Fig. 2(b), the light field of the single MR ($|E_{\text{s}}|$) has the same amplitude in every resonance peak, and the spectrum interval of two adjacent peaks is equal to the FSR of a typical MRR. Meanwhile, the amplitude of the feedback-interferential light field ($|E_{\text{f}}|$) maintains the same every other peak, and every two adjacent $|E_{\text{f}}|$ are inverted. It is also seen that the two light fields interfere at each resonance wavelength, as shown in Fig. 2(c). Thus, the amplitudes with overlarge peaks of E_{f} are eliminated at one of every two resonances of typical MRR by the peaks of E_{s}, and the other resonant dips of E_{f} are strengthened with a larger extinction ratio by the interferential E_{s}. Thus, the output spectrum of feedback MRR has a larger quasi-FSR than the typical single-ring MRR.

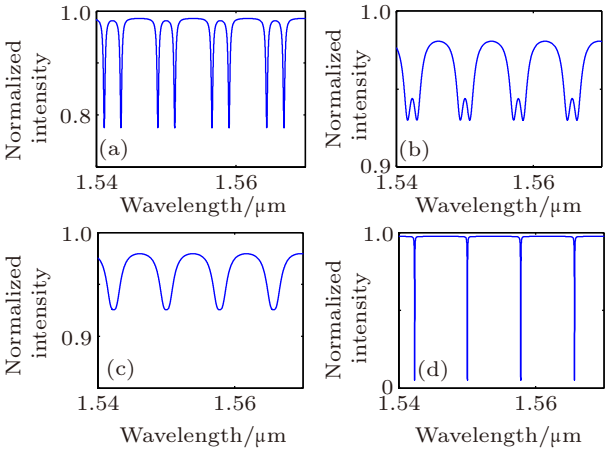


Fig. 4. (color online) Relationship between the output spectrum of feedback MRR and the coupling coefficient κ. (a) $\kappa = 0.9$, (b) $\kappa = 0.6$, (c) $\kappa = 0.53$, and (d) $\kappa = 0.1$.

Furthermore, in order to obtain the output spectral response of feedback MRR, it is important to select an appropriate coupling coefficient κ. The relationship between the output spectrum of feedback MRR and κ is shown in Fig. 4. There are two resonant dips in each quasi-FSR when strong coupling occurs (κ is large enough), such as $\kappa = 0.9$ or 0.6, as shown in Figs. 4(a) and 4(b). Two dips will become only one dip in every period when κ is close to 0.53. When κ keeps on decreasing, the resonant dips will become sharp, and its ER can be much higher, as shown in Figs. 4(c) and 4(d). Since the loss of MR is usually small, small κ should be selected to obtain the spectrum with appropriately high Q and large ER according to the critical coupling condition. Therefore, the output spectrum of feedback MRR with one sharp and high ER resonant dip in every period can be obtained. Thus, the quasi-FSR is twice as much as the FSR of the conventional MRR in the weak coupling case (the length of the feedback waveguide is equal to the perimeter of the ring). Hence, the measurement rang of the proposed sensor can be much larger according to Eq. (6).

In the following, the transmission spectrum at the Mach–Zehnder interferential output port is analyzed on the basis of previous discussion. Here, the operating wavelength λ_{c} is 1550 nm. We choose the order of the microring $m_1 = 400$ corresponding to the radius of the reference ring $R_{\text{r}} = 40.276$ μm, and $m_2 = 410$ with the radius of the sensing ring $R_{\text{s}} = 41.283$ μm. The length of the feedback waveguide of each feedback MRR is equal to the perimeter of its ring, respectively. The spectral response of the sensing ring will shift when the analyte is presented, while the reference ring's spectrum remains stable. Thus, the overlap wavelength will change, which means that the central resonance will shift at the output port.

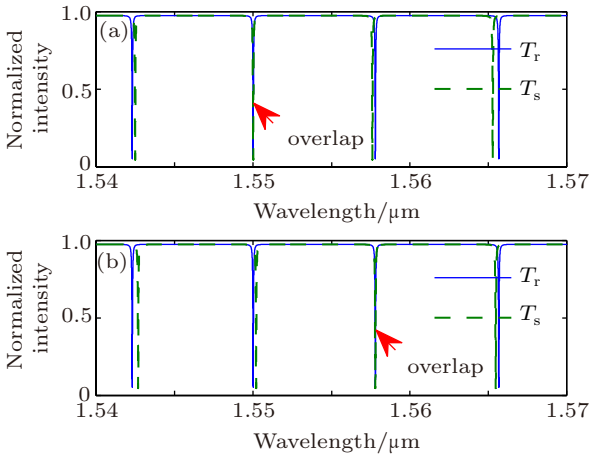


Fig. 5. (color online) Two spectral response (T_{r} for the reference ring, T_{s} for the sensing ring). (a) Absence of analyte and (b) presence of analyte.

As shown in Fig. 5(a), two resonances (T_{r} and T_{s}) overlap at $\lambda_1 = 1550$ nm without the analyte. In this case, we choose the analyte with the corresponding minimum measurable index-change $\Delta n_{\text{eff}} = 1.22 \times 10^{-4}$ RIU. When the analyte is present, the spectral response T_{s} shifts $\Delta\lambda_{\text{s}} = \Delta\text{FSR}_{\text{Q}} = 0.19$ nm, while T_{r} is stable. The overlap resonance changes to $\lambda_2 = 1557.75$ nm, as shown in Fig. 5(b). In the presence of analyte, the whole transmission spectrum shifts, as shown in Fig. 6(b). At this time, the central resonance jumps to λ_2. $\Delta\lambda\,(= \lambda_2 - \lambda_1 = 7.75$ nm) is the variation of central resonance

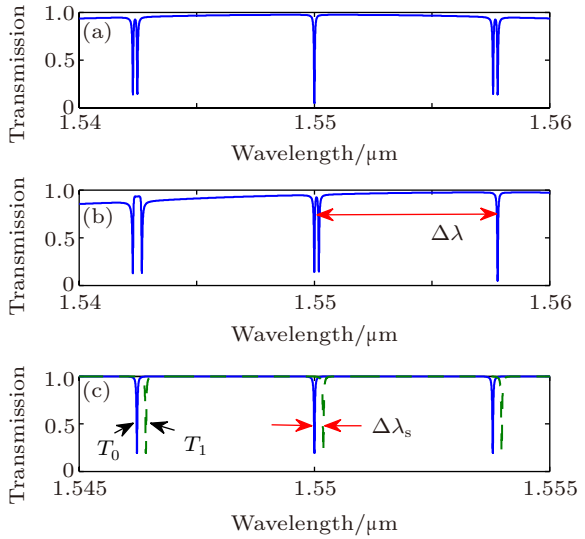


Fig. 6. (color online) Transmission spectra at the output port (a) in the absence of analyte and (b) in presence of analyte; (c) transmission spectra of a conventional single-ring MRR in absence of analyte T_0 (solid line), and in presence of analyte T_1 (dashed line).

in the output spectrum for the whole structure, while $\Delta\lambda_s$ is the variation of the spectral response T_s, which can also represent the spectral change of a conventional single-ring MRR under the same index-change, as shown in Fig. 6(c). Hence, the sensitivity of the proposed sensor (S) is much higher than that of a conventional sensor (S_c), and the improvement factor of sensitivity $F_a = S/S_c = \Delta\lambda/\Delta\lambda_s = 40.79$. When the effective refractive index of analyte changes more than the minimum measurable Δn_{eff} with discrete modality, the output spectral response will shift multiple quasi-FSR of the reference feedback MRR, which is helpful for sensing with a low-resolution detecting instrument since $\Delta\lambda$ is at the scale of nanometer. Moreover, as seen from Figs. 6(a) and 6(b), we measure the index variation by judging the shift of central resonance. It is known in the conventional MRR that low quality factor Q means wider resonance dips in the spectrum, which may be difficult to distinguish when two such dips are close. Unlike the conventional MRR, we detect the central resonance in this proposed sensor. The central resonance locates at the position of the peak in one period of the Mach–Zehnder interference. Since the period of the Mach–Zehnder interference is much larger than the quasi-FSR, it is easier to distinguish the central resonance from the symmetric split dips around. At this time, spectrum with relatively low Q (wider resonance troughs) can also be detected exactly, so the Q factor is not as critical as that in the conventional case. In order to realize a broad measurement range of the analyte's index-change, it can be expected that the observed wavelength range in the actual case will be much broader than that in simulation (1540 nm to 1560 nm).

4. Conclusion

In summary, a novel digital optical sensor with high sensitivity and large measurement range has been proposed. The structure consists of two feedback MRRs. The spectral responses of the two MRRs mutually interfere to form the whole spectrum at the output port. The spectral response of individual feedback MRR through the TMM approach has been deduced, and the related simulation has been carried out. It can be found that when the feedback waveguide's length is equal to the perimeter of the ring in the weak coupling case, the proposed sensor has a large measurement range compared to the conventional sensor due to its great dependence on the quasi-FSR. Meanwhile, the sensitivity of the proposed sensor can be many times higher than that of a comparable conventional sensor. Since the detection principle is based on the shift of central resonance, the high Q factor is not critical.

References

[1] Kwon M S and Steier W H 2008 *Opt. Express* **16** 9372
[2] Yalcin A, Popat KC, Aldridge J C and Goldberg B B 2006 *IEEE J. Sel. Top. Quantum Electron* **12** 148
[3] Ashkenazi S, Chao C Y, Guo L J and Odonnell M 2004 *J. Appl. Phys.* **85** 5418
[4] Su B, Wang C and Chen H 2011 *J. Lightwave Technol.* **29** 1535
[5] Chao C Y, Fung W and Guo L J 2006 *IEEE J. Sel. Top. Quantum Electron* **12** 134
[6] Mo W, Zhou Z, Wu H and Gao D 2011 *IEEE Sens. J.* **11** 1035
[7] De Vos K, Bartolozzi I, Schacht E, Bienstman P and Baets R 2007 *Opt. Express* **15** 7610
[8] Xia Z X, Yao C and Zhou Z P 2008 *IEEE J. Quantum Electron* **44** 100
[9] Chen L, Sherwood-Droz N and Lipson M 2007 *Opt. Lett.* **32** 3361
[10] Xia F, Sekaric L and Vlasov Y 2007 *Nat. Photon.* **1** 65
[11] Huang Q Z, Yu J Z, Chen S W, Xu X J, Han W H and Fan Z C 2008 *Chin. Phys. B* **17** 2562
[12] Li X, Zhang Z, Qin S, Wang T, Liu F, Qiu M and Su Y 2009 *Appl. Opt.* **48** F90
[13] Yi H, Citrin D and Zhou Z 2011 *J. Opt. Soc. Am. B* **28** 1611
[14] Zhou L and Poon A 2007 *Opt. Lett.* **32** 781
[15] Dai D 2009 *Opt. Express* **17** 23817
[16] Claes T, Bogaerts W and Bienstman P 2010 *Opt. Express* **18** 22747
[17] Dai D and He S 2009 *J. Opt. Soc. Am. B* **26** 511
[18] Poon J, Scheuer J, Mookherjea S, Paloczi G, Huang Y and Yariv A 2004 *Opt. Express* **12** 90
[19] Cho S and Soref R 2008 *Opt. Express* **16** 13304
[20] Tian H, Zhang Y D, Wang H, Ouyang Q Y, Wang N and Yuan P 2009 *Chin. Phys. B* **18** 221
[21] Zhou L and Poon A 2007 *Opt. Express* **15** 9194